



Universidad Autónoma  
de Madrid

**Biblos-e Archivo**  
Repositorio Institucional UAM

**Repositorio Institucional de la Universidad Autónoma de Madrid**

<https://repositorio.uam.es>

Esta es la **versión de autor** del artículo publicado en:

This is an **author produced version** of a paper published in:

Waste Management 142 (2022): 9-18

**DOI:** <https://doi.org/10.1016/j.wasman.2022.02.003>

**Copyright:** © 2022 Elsevier Ltd. This manuscript version is made available under the CC-BY-NC-ND 4.0 licence <http://creativecommons.org/licenses/by-nc-nd/4.0/>

El acceso a la versión del editor puede requerir la suscripción del recurso

Access to the published version may require subscription

# Improved energy recovery from food waste through hydrothermal carbonization and anaerobic digestion

Gemma Mannarino<sup>a,b,\*</sup>, Andrés Sarrión<sup>a</sup>, Elena Diaz<sup>a</sup>, Riccardo Gori<sup>b</sup>, M. Angeles de la Rubia<sup>a</sup>, Angel F. Mohedano<sup>a</sup>

<sup>a</sup> *Department of Chemical Engineering, Universidad Autónoma de Madrid, Campus de Cantoblanco, 28049 Madrid (Spain)*

<sup>b</sup> *Department of Civil and Environmental Engineering, University of Florence, via di S. Marta 3, 50139 Florence (Italy)*

\*Corresponding author: Email: gemma.mannarino@unifi.it (G. Mannarino)

## Abstract

Here we studied energy valorization of food waste by hydrothermal carbonization coupled with anaerobic digestion. Hydrothermal treatment was carried out at 200°C and 230°C for 1 h, obtaining hydrochar with properties suitable for solid biofuel according to ISO/TS 17225-8. The increase in temperature improved the fuel properties of hydrochar (higher heating value 20.3 and 23.7 MJ kg<sup>-1</sup>, fuel ratio 0.33 and 0.37, energy density 1.07 and 1.25). The anaerobic digestion of process water achieved methane yields around 150 mL CH<sub>4</sub> STP g<sup>-1</sup> COD<sub>added</sub> and made it possible to remove some specific recalcitrant compounds, such as 2-methylpyridine and 2-ethyl-3-methylpyrazine. Energy recovery from hydrochar and process water seems to be an interesting alternative way to sustain the process energetically and economically, despite the significant energy inputs required for hydrothermal carbonization.

**Keywords:** anaerobic digestion; biofuel; energy recovery; food waste; hydrothermal carbonization.

24    **Abbreviation list**

25    AD, anaerobic digestion;

26    CCI, comprehensive combustion index;

27     $E_{\text{input}}$ , energy input;

28     $E_{\text{output}}$ , energy output;

29    FC, fixed carbon;

30    FW, food waste;

31    GC/MS, gas chromatography-mass spectrometry;

32    HC, hydrochar;

33    HHV, higher heating value;

34    HTC, hydrothermal carbonization;

35    PA, partial alkalinity;

36    PW, process water;

37    SCOD, soluble COD;

38    SMP, specific methane production;

39    TA, total alkalinity;

40    TAN, total ammonia nitrogen;

41    COD, chemical oxygen demand;

42    TN, total nitrogen,

43 TOC, total organic carbon;

44 TP, total phosphorus;

45 TS, total solids;

46 TVFA, total volatile fatty acids;

47 VFA, volatile fatty acids;

48 VM, volatile matter;

49 VS, volatile solids;

50  $Y_{HC}$ , hydrochar yield;

51  $Y_{PW}$ , process water yield.

52

53

54

55

56

57

58

59

60

61

## 1. Introduction

Food waste (FW) is organic waste derived from any stage of the food supply chain and it is a significant fraction of municipal solid waste. More than 2000 million tons of municipal waste were generated worldwide and production is estimated to increase by 70% to 2050.

In Europe, current legislation focuses on reducing food waste and promotes actions to minimize its impact on the environment through the so-called circular economy (European Commission, 2020). Indeed, many EU countries have limited the disposal of food waste in landfills, supporting effective segregation at the source and therefore facilitating its valorization (Browne and Murphy, 2013).

As a rule, FW management can be based on biological technologies and thermochemical pathways. Regarding biological treatment, anaerobic digestion (AD) has many applications, as it can convert a significant amount of FW into biogas, potentially upgradable to bio-methane, with appreciable environmental benefits. On the other hand, anaerobic digestion is characterized by long treatment times (up to 30–40 days) and the process can be inhibited by high concentrations of free ammonia ( $\text{NH}_3$ ) and cations (Pham et al., 2015). Thermochemical conversions are another feasible route for handling food waste. Incineration is a mature technology capable of converting wastes into heat and energy, but it usually requires feedstock pre-treatments (FW is by far the wettest fraction of municipal solid wastes) and it has atmospheric emissions which generally contain dioxins and heavy metals (Pham et al., 2015; Saqib et al., 2019) requiring additional treatment of the gases produced. In this framework, hydrothermal carbonization (HTC) emerges as an environmentally friendly and energy-efficient

sustainable technology, as it can be used to treat FW to obtain a product with attractive energy properties for co-firing coal (Gupta et al., 2020). Hydrothermal carbonization is an exothermic process in which the wet feedstock is treated at 170–250°C for short times (5–240 min) under self-generated pressure. Through hydrolysis, condensation, aromatization, dehydration and decarboxylation reactions, three fractions are obtained: a solid carbonaceous product named hydrochar, process water rich in sugars and organic compounds, and a small gaseous fraction consisting mainly of CO<sub>2</sub> (Funke and Ziegler, 2010).

Hydrochar derived from FW is a valuable product with a high carbon content (45–93%) and energy values in the range 15–30 MJ kg<sup>-1</sup> (Saqib et al., 2019). Lu et al. (2012) carried out hydrothermal carbonization of FW in a batch reactor at 250°C and found that the potential energy generation of HTC of food waste was higher than that recovered by landfilling, composting, AD or incineration. Evaluations of different HTC conditions in the conversion of FW to solid fuel have been reported in the literature. Akarsu et al. (2019) performed HTC of food waste at different temperatures (175–250°C) and with different reaction times (15–120 min), obtaining optimal conditions in terms of mass and energy efficiency at 200°C and 60 min. On the other hand, Li et al. (2020) compared the total energy recoverable from hydrochar resulting from different organic wastes as a function of HTC conditions, reporting that the highest energy generation (~17.5 MJ kg<sup>-1</sup><sub>dry feedstock</sub>) was obtained from food waste at less than 200°C for less than 150 min.

Since process water from HTC contains water-soluble organic compounds (Funke and Ziegler, 2010), its valorization through AD is a promising approach. While AD of organic wastes is a mature technology, its application to process water from food waste

carbonization is new. Lucian et al. (2020) recently investigated application of HTC to the organic fraction of municipal solid waste and found that coupling AD of process water with hydrochar combustion is an energy-efficient combination. Aragón-Briceño et al. (2017) used the liquid fraction obtained after HTC of sewage sludge digestate at 160–250°C for 30 min to obtain biogas by AD, also adding the resulting hydrochar to the medium, which delayed the generation of volatile fatty acids and improved the CH<sub>4</sub> production rate. On the other hand, Marin-Batista et al. (2020a; 2020b) hydrothermally carbonized cow manure and digestate at 170–240°C for 1 h, evaluating energy recovery from AD of process water and combustion of hydrochar. For dairy manure carbonized at 170°C and 200°C, the energy recovery yield was at least 80% of feedstock energy content (Marin-Batista et al., 2020b).

The main aim of this study was to explore the energy valorization of FW by hydrothermal carbonization coupled with anaerobic digestion of the process water, and combustion of the hydrochar. Hydrothermal carbonization of FW was carried out at 200°C and 230°C. Then hydrochar was characterized to define its combustion properties. The time-course of AD of process water was investigated, monitoring parameters such as organic matter, volatile fatty acids and recalcitrant compounds. Lastly, we calculated the energy balance of coupling hydrothermal carbonization and AD, taking the energy content of the hydrochar into account.

## **2. Materials and methods**

### ***2.1. Food waste***

Food waste was collected from a local management plant that operates in a food supply distribution platform (Madrid, Spain). The raw food waste, which mainly

consisted of fruit and vegetables, was ground and frozen in 1.5 kg portions at -20°C to facilitate conservation, while a sample was oven dried at 105°C for 24 h prior to analysis of its composition (Table 1). In each experiment, moisture of thawed FW portions was measured (91–93 wt.%). The main characteristics of the feedstock (average of n=3 portions with standard deviations in brackets) were: total solids (TS) 88.2 (2.8) g kg<sup>-1</sup>, volatile solids (VS) on TS 87.6 (0.2) % and total chemical oxygen demand (COD) wet basis 102.2 (2.0) g O<sub>2</sub> kg<sup>-1</sup>.

## ***2.2. Hydrothermal carbonization***

Hydrothermal carbonization of food waste was conducted, by triplicate, in an electrically heated, stirred ZipperClave pressure vessel (4 L). In each experiment, the reactor was loaded with 1.5 kg defrosted food waste. The operating temperatures (200°C and 230°C) were reached by heating the reactor at 3 °C min<sup>-1</sup> and holding for 1 h. The reaction was stopped by cooling at 2.5 °C min<sup>-1</sup> with an internal heat exchanger using tap water. The resulting slurry (a mixture of hydrochar and process water) was separated by filtration with a 250 µm membrane vacuum filter. The hydrochars (HC200, HC230) were obtained by oven-drying the solid fraction overnight at 105°C, followed by grinding and sieving to a particle size between 100 and 200 µm. The process water (PW200, PW230) was filtered with 0.45 µm Scharlab glass filters and stored at 4°C.

## ***2.3. Anaerobic digestion experiments***

Anaerobic digestion experiments were performed on food waste, PW200 and PW230. Batch-wise AD tests were carried out in 120 mL glass serum vials, filled with 60 mL suspension of inoculum, substrate (raw food waste or process water from HTC), deionized water and a basal medium with macro- and micronutrients, as reported



elsewhere (Villamil et al., 2018). Granular anaerobic sludge from a brewery wastewater treatment plant was used as inoculum. It was characterized (average of n=3 samples with standard deviations in brackets) as follows: TS 53.7 (0.9) g L<sup>-1</sup>, VS 46.2 (0.9) g L<sup>-1</sup> and COD 33.1 (2.0) g O<sub>2</sub> L<sup>-1</sup>. The initial inoculum concentration was set at 15 g VS L<sup>-1</sup> and the inoculum-to-substrate ratio at 2 on a COD basis as recommended by Villamil et al. (2018). The vials were sealed with rubber stops and metal crimps, and were flushed with N<sub>2</sub> for 3 min to ensure anaerobic conditions. The vials were kept under mesophilic conditions (35 ± 1 °C) in a thermostatic shaking water bath at 100 rpm. Anaerobic digestion was monitored using ten vials for each process water: three for biogas measurements (volume and composition), and the other seven were sacrificed during the experiment to monitor digestion parameters over time. Only three AD runs were performed on food waste to measure biogas. Triplicate blank samples with no substrate were run to determine the background methane yield of the inoculum, and triplicate control experiments were also performed on starch to evaluate the methanogenic activity of microorganisms. Methane yield was calculated by subtracting the amount of methane produced by blanks, and methane volume at STP (0°C, 1 atm) was recorded.

#### ***2.4. Analytical methods***

The elemental composition (C, H, N and S) of the hydrochar and process water samples was determined on a CHNS analyzer (LECO CHNS-932). Proximate analysis was done according to ASTM methods D3173-11, D3174-11 and D3175-11 to determine moisture, ash, volatile matter (VM) and fixed carbon (FC) (by difference), respectively, of the hydrochar. Oxygen content was calculated by difference. The higher heating value (HHV) of dried solid samples was estimated by Eq. (1), which is a unified

correlation to calculate the HHV from C, H, N, S, O and ash content according to Channiwala and Parikh (Channiwala and Parikh, 2002):

$$HHV (MJ kg^{-1}) = 0.349 C + 1.178 H + 0.100 S - 0.103 O - 0.015 N - 0.021 Ash$$

(1)

Analysis of variance was performed using the MINITAB® software. Means were compared using Welch's test.

The concentration of other inorganic elements in hydrochar and process water was quantified by inductively coupled optical emission spectroscopy (ICP-OES) on an IRIS INTREPID II XDL instrument (ThermoFisher Scientific).

Inoculum and process water of AD tests were characterized by measuring TS and VS according to standard methods 2540B and 2540E (APHA, 2005), and COD by the method of Raposo et al. (2008). Sacrificed samples were filtered (0.45 µm) and analyzed to determine: pH (Crison 20 Basic pH meter), partial and total alkalinity (PA and TA) by pH titration to 5.75 and 4.3, respectively (Jenkins et al., 1983), soluble COD (SCOD) applying the closed digestion and colorimetric standard method 5220D, and total ammonia nitrogen (TAN) by distillation and titration according to standard method 4500-NH<sub>3</sub> (APHA, 2005). Total organic carbon (TOC) was determined using an OI Analytical TOC analyzer (model 1010, Texas, USA). Individual volatile fatty acid (VFA) concentrations (C2-C7, including isoforms) were identified by gas chromatography (GC) in a Varian 430-GC instrument as described elsewhere (De la Rubia et al., 2018a). Individual chemical species were identified by GC-MS (CP-3800/Saturn 2200 with Varian CP-8200 autosampler injection) (De la Rubia et al., 2018a). The NIST 2018 Library was used to assess compounds. Only compounds with a

probability of at least 50% were considered. Biogas production was determined using a manometric method, measuring the pressure increase in each vial with an electronic pressure monitor (ifm, PN 7097) (De la Rubia et al., 2018b). Biogas composition (H<sub>2</sub>, H<sub>2</sub>S, CO<sub>2</sub> and CH<sub>4</sub>) was measured by gas chromatography, using a Bruker 450-GC (Goes, The Netherlands) (De la Rubia et al., 2018a). Biogas was subsequently exhausted to re-establish atmospheric pressure.

## 2.5. Calculations

Hydrochar mass yield (Y<sub>HC</sub>), i.e., the weight ratio of hydrochar recovered (W<sub>HC</sub>) to food waste feedstock (W<sub>FW</sub>) on a dry basis, was calculated with Eq. (2):

$$Y_{HC}(\%) = \left( W_{HC} / W_{FW} \right) \cdot 100 \quad (2)$$

Likewise, the process water yield (Y<sub>PW</sub>) expresses the mass ratio of total solids in process water (W<sub>PW</sub>) to that of food waste (W<sub>FW</sub>) on a dry basis, and was calculated with Eq. (3):

$$Y_{PW}(\%) = \left( W_{PW} / W_{FW} \right) \cdot 100 \quad (3)$$

The energy recovery efficiency was calculated with Eq. (4):

$$\text{Energy recovery efficiency} = Y_{HC} \cdot \frac{HHV_{HC}}{HHV_{FW}} \quad (4)$$

where the HHV<sub>HC</sub> and HHV<sub>FW</sub> are the higher heating values of hydrochar and food waste, respectively.

A more in-depth evaluation for the combustion performance is carried out from the comprehensive combustion index (CCI). The hydrochar CCI was calculated using Eq. (5) (Marin-Batista et al., 2020b):

$$CCI(\text{min}^{-2} \cdot ^\circ\text{C}^{-3}) = \frac{DTG_m \cdot DTG_{mean}}{T_i^2 \cdot T_b} \quad (5)$$

where  $DTG_m$  and  $DTG_{mean}$  are the maximum and the average rate of weight loss, respectively, and  $T_i$  and  $T_b$  are the ignition and the burnout temperatures, respectively. High values of the CCI indicate a satisfactory combustion performance by an easy ignition and an efficient burnout (Mureddu et al, 2018).

The specific methane production (SMP,  $\text{Nm}^3 \text{CH}_4 \text{ kg}^{-1} \text{COD}$ ) obtained from batch anaerobic tests was converted into  $HHV_{PW}$  values using Eq. (6):

$$HHV_{PW}(\text{MJ kg}^{-1}) = 39.8 \cdot \text{SMP} \cdot \text{COD} / \text{TS} \quad (6)$$

where the coefficient 39.8 is the higher heating value for pure methane ( $\text{MJ Nm}^{-3}$ ), and  $\text{COD TS}^{-1}$  is the COD to TS ( $\text{kg COD kg}^{-1} \text{TS}$ ) in the PW.

Lastly, the total potential energy recovery was estimated with Eq. (7):

$$\text{Energy recovery} (\text{MJ kg}_{dry\ feedstock}^{-1}) = (HHV_{HC} \cdot Y_{HC}) + (HHV_{PW} \cdot Y_{PW}) \quad (7)$$

where  $HHV_{HC}$  is the HHV ( $\text{MJ kg}^{-1}$ ) of hydrochar estimated with Eq. (1).

### 3. Results and Discussions

#### 3.1. Hydrochar as solid biofuel

Table 1 collects the mean values and standard deviation of mass yield, proximate and ultimate analyses, and HHV of the raw food waste and hydrochars. Carbonization temperature showed a significant effect ( $p < 0.001$ ) on mass yield, fixed carbon, volatile matter, ash content, and HHV. The C, N and O content were also significantly ( $p < 0.05$ ) influenced by HTC temperature. The hydrochar yield decreased greatly at both HTC temperatures, due to the subcritical state of water induced above  $200^\circ\text{C}$ , which

results in the transfer of components (such as proteins, amino acids and sugars) from the feedstock to the process water. This occurs at high temperatures and short reaction times (Lu et al., 2012). The raw food waste had a low fixed carbon content, since it is mainly composed of organic compounds such as sugars, carbohydrates and proteins, and this low fixed carbon is also related to its high volatile content. The FC content in the hydrochars increased in comparison with raw feedstock, increasing the firing temperature and providing greater flame stability during combustion of these materials. High fuel ratio values maintain a less violent flame and reduce heat loss during combustion (He et al, 2013). This allows hydrochar to be used as fuel in power plants, blended with coal, reducing the fossil fuel contribution to CO<sub>2</sub> emissions (Marin-Batista et al., 2020b). On the other hand, the ash content in hydrochar increased with temperature due to transfer of organic matter to the process water and to the high sample content of inorganic compounds, which remain in the solid phase after hydrothermal treatment (Reza et al., 2013). The increase in ash content in hydrochar is the most concerning issue for its application as a solid fuel. Ro et al. (2019) highlighted the potential of hydrochar as a renewable fuel in existing coal-fired power plants and concluded that, although fossil coals cannot be replaced entirely with hydrochar, blending up to 10% hydrochar with coal does not affect the combustion characteristics or the amount of ash for existing power plants. To reduce the ash content of hydrochar, some works have studied the blending of high-ash biomasses with other hydrochar precursors (e.g., lignocellulosic wastes) prior to HTC (He et al., 2019; Lang et al., 2019; Zheng et al., 2019). Some studies have used acidic reagents, mainly HCl, in the HTC process to favor the extraction of the inorganic content to the process water (Dai et al., 2017; Sarrion et al., 2021).

Table 1 also shows the mean values of some elements in the ash fraction of food waste and hydrochars, the most abundant being P and metals such as Na, K, Ca, Mg, Fe and Al. HTC temperature had a significant effect on P and metal content ( $p < 0.001$ ). It can be observed that except for K and Na, which decreased in amount at higher temperature, metals mainly remained in the hydrochar. Alkali metals (K and Na), responsible for fouling, are generally transferred to the process water under severe carbonization conditions (Wang et al., 2019). In addition, the reduction of alkali metals and the increase in alkaline earth metals (Mg and Ca) promote ash with a high melting temperature, which is easier to remove from furnaces and boilers after combustion (Smith and Ross, 2016).

An increase in HTC temperature generated hydrochars whose O/C and H/C atomic ratios were lower than those of raw food waste (0.56 and 1.64, respectively), indicating that the degree of hydrochar carbonization was improved by the dehydration, carboxylation and condensation reactions (Akarsu et al., 2019). Thus, HC200 achieved H/C (1.41) and O/C (0.52) atomic ratios comparable to those of peat, while HC230 gave atomic ratios (1.34 and 0.4, respectively) comparable to those of lignite.

#### **Table 1**

Thermogravimetric analysis (TGA) was used to determine the combustion characteristics of feedstock and hydrochar (Fig.1). The TG and first derivative (DTG) curves provide information on the thermal degradation patterns of food waste, indicating an initial mass loss up to 120°C, related to moisture evaporation. Thermal decomposition of food waste and hydrochar started at temperatures below 150°C due to the low thermal stability of sugars, resulting in an ignition temperature ( $T_i$ ) of hydrochar

that increased slightly from 184 to 190°C. Subsequently, the highest DTG peak or maximum weight loss rate ( $T_m$ ) was associated with combustion of the samples and was found for all samples at temperatures around 280–300°C, being higher for hydrochars obtained at higher temperatures. Before reaching this combustion peak, another earlier peak (180–220°C) was observed only in the feedstock and HC200, related to the greater solid matrix destruction of the light carbon structures (Wang et al., 2018), and indicating that volatile matter in HC230 was largely reduced. Subsequently, a second pronounced DTG peak was recorded at 390–500°C, attributed to the combustion of more stable structures with high molecular weight together with fixed carbon (Niu et al., 2016), the width (combustion temperature range) of which also increased with HTC temperature. A third peak was observed at 480°C with HC230 due to combustion of the remaining fixed carbon.

### **Figure 1**

The combustion characteristics of the hydrochars are shown in Supplementary information (Table S1). The  $T_i$  and the burnout temperature ( $T_b$ ) increased and decreased, respectively, with HTC temperature, decreasing the  $T_m$  and resulting in hydrochar with a low CCI index ( $\sim 10 \cdot 10^{-7} \text{ min}^{-2} \text{ }^\circ\text{C}^{-3}$ ) (Eq. (6)), confirming high combustion as the reactivity of hydrochar increased (Niu et al., 2016). A positive effect of temperature on HHV was observed, improving that of the feedstock, and reaching typical brown-coal values at the higher HTC temperature. Compared to the initial feedstock, the fuel ratio (FC/VM) of hydrochar doubled at the higher temperature due to the loss of volatile compounds during HTC. This indicated generation of hydrochar richer in fixed carbon, which is determinant for improving combustion performance as solid fuel and reducing emission of pollutants (Wang et al., 2019). The hydrochar fuel

ratio was also less than 2.5, which is decisive for qualifying it as solid fuel suitable for pulverized combustion systems (Sahu et al., 2010). The energy density of hydrochar increased with HTC temperature, and considering the initial performance of food waste to hydrochar, the higher HTC temperature (230°C) resulted in slightly more efficient energy recovery.

Fuel properties are fundamental for the viability of hydrochar as a solid fuel. Hydrochar was analyzed to check its compliance with ISO/TS 17225-8 for thermally treated and densified biomass. This standard establishes specific limits for pellets, obtained by thermal processing of non-woody biomass, to be used as solid biofuels. As there is no specific standard for solid fuel derived from food waste and since the food waste used as feedstock in this study was mainly from fruit and vegetables, the hydrochar characteristics were compared with the specification of property class TA3 for fruit biomass. The two hydrochars (Table 1) complied with the limits defined by the standard:  $N < 2.5\%$  and  $S < 0.3\%$ . No requirements are defined for ash, volatile matter, specific metals (e.g., Cd, Cr, Cu, Pb and Ni) or net calorific value for TA3. Nevertheless, the high HHV of both hydrochars ( $> 20 \text{ MJ kg}^{-1}$ ) suggests that their use as biofuels in industry is feasible, HC230 showing the best results.

### ***3.2 Mesophilic anaerobic digestion of process water***

The characteristics of process water samples obtained by HTC of food waste at 200 and 230°C (given as average values of three determinations with standard deviations in brackets) are reported in Table 2.

### **Table 2**



The SCOD values are consistent with ranges described in the literature, which are slightly lower than those reported for process water from carbonization of food waste from a student hostel (68–97 g O<sub>2</sub> L<sup>-1</sup>) at 200°C for 0.5–5 h (Gupta et al., 2020), and relatively higher than PW from HTC of the organic fraction of municipal solid waste (40–45 g O<sub>2</sub> L<sup>-1</sup>) at 180–250°C for 1–6 h (Lucian et al., 2020).

A decreasing trend of TS was observed with increasing temperatures, while the VS/TS ratio remained constant. Acid pH was found for both process water samples. Gupta et al. (2020) reported similar pH values for HTC process water from food waste (3.3–3.9). These pH values are consistent with the formation of a variety of organic acids during the hydrothermal process (Funke and Ziegler, 2010).

TOC concentrations were comparable to those reported in the literature. Gupta et al. (2020) observed a decreasing trend of TOC (from 42 to 21 g L<sup>-1</sup>) with increasing HTC reaction time (0.5–5 h) for process water derived from food waste carbonized at 200°C. The TN concentrations are slightly lower than those (2.4–4.7 g L<sup>-1</sup>) reported for spent liquor obtained from HTC of food waste at 200°C (15–120 min) (Akarsu et al., 2019). Phosphorus concentrations in process water decreased significantly with increasing temperature. This trend was similar to the pattern observed by Idowu et al. (2017) during hydrothermal carbonization of food waste to recover nutrients, due to precipitation of phosphorus with cations (e.g., Ca, Mg, Fe and Al) and/or integration into hydrochar via sorption.

Fig. 2a, 2b show the individual time-course of VFA during anaerobic digestion of PW200 and PW230, respectively. Acetic acid (C<sub>2</sub>) accounted for about 50% of total volatile fatty acids (TVFA) (in mg acetic acid L<sup>-1</sup>) for the two process waters in the

early stage. In contrast, low concentrations of longer chain VFA, such as valeric (C5), isovaleric (i-C5), caproic (C6) and isocaproic (i-C6), were measured in both samples (<150 and <100 mg acetic acid L<sup>-1</sup>, for the sum of C5 and i-C5 and for the sum of C6 and i-C6, respectively). Small amounts of butyric (C4) and iso-butyric (i-C4) were also detected in both process waters. During AD, the concentration of TVFA showed a decreasing trend until day 15, indicating an efficient acidogenic-acetogenic stage. At day 15, TVFA concentrations, 143 (6) and 186 (2) mg acetic acid L<sup>-1</sup> for PW200 and PW230, resulted in overall reductions in TVFA of 81% and 65%, respectively. These considerable reductions in VFA concentrations show that the methanogenic phase was effective in the first 15 days, indicating a correct balance between hydrolysis and methanogenic rate. From Day 22, TVFA concentrations in PW200 samples showed a slight increase with respect to the TVFA concentration at Day 15 until the end of the experiment. In the case of PW230, TVFA concentrations remained almost constant until the end of AD tests. However, no relevant differences were detected between PW200 and PW 230 samples in the TVFA profile. In fact, the TVFA concentration showed values in the range of 150 – 350 mg acetic acid L<sup>-1</sup> in both cases, starting from Day 2. These TVFA trends suggested that a good balance was reached between TVFA production/consumption producing CH<sub>4</sub>.

Fig. 2c shows the time-course of SCOD (in g O<sub>2</sub> L<sup>-1</sup>) and the TVFA/SCOD ratio (%) (both parameters expressed as g O<sub>2</sub> L<sup>-1</sup>). Soluble COD of both process waters gradually decreased in the first 15 days, due to conversion of soluble organic matter to methane. It then remained almost constant until the end of the experiment, suggesting the presence of a non-biodegradable SCOD fraction. A slight increase in SCOD was observed in the latter stages of AD for PW200. The TVFA to SCOD ratio was around 20% for both

process waters in the early stages of AD, indicating effective conversion of TVFA. About 30% of TVFA in SCOD remained constant in the last stages of AD for both process waters (Fig. 2c), which may support the hypothesis of the presence of refractory compounds.

## **Figure 2**

Parameters such as pH, TA and TAN are key factors for assessing the evolution of AD. For both runs, pH varied in the range 7.4–7.9. These pH values are compatible with the growth of anaerobic microorganisms (De la Rubia et al., 2018b). TA reached values above 4.0 g CaCO<sub>3</sub> L<sup>-1</sup> at the end of the experiment for both process waters, which allowed the system to provide enough buffering capacity (Villamil et al., 2018). TAN was in the range 0.2–0.3 g N L<sup>-1</sup> in the early stages, increasing to 1 and 0.8 g N L<sup>-1</sup> for PW200 and PW230, respectively, in the last stage. These TAN values are lower than the inhibitory concentration 1.7 g N L<sup>-1</sup> (De la Rubia et al., 2018b). These aspects could support that AD approach is promising for treating HTC-derived process water. Indeed, although this specific study was limited to batch test assays, some other works have assessed that the continuous operation of AD on HTC-derived process water from different biomasses (e.g., sewage sludge) can be successfully developed (Liu et al., 2021; Weide et al., 2019; Wirth et al., 2015). Particularly, Liu et al. (2021) reported 71 % COD removal and 285 mL CH<sub>4</sub> STP g<sup>-1</sup> COD<sub>added</sub> can be achieved by operating an upflow anaerobic sludge blanket reactor (UASB) for 180 days using HTC-derived PW from sewage sludge.

Methane yield grew exponentially from the early stage to day 20 for all runs. The final methane yields were 140 (7) and 154 (4) mL CH<sub>4</sub> STP g<sup>-1</sup> COD<sub>added</sub> for PW200

and PW230, respectively. These methane productions were comparable to the yields reported for process water from carbonized sewage sludge (144–177 mL CH<sub>4</sub> STP g<sup>-1</sup> COD<sub>added</sub>) by Villamil et al. (2018). Cumulative methane yields at the end of the experiment proved comparable for both runs, slightly higher for PW230, while food waste showed higher methane production (228 (10) mL CH<sub>4</sub> STP g<sup>-1</sup> COD<sub>added</sub>). Lower methane yield (194 (1) mL STP CH<sub>4</sub> g<sup>-1</sup> COD<sub>added</sub>) was reported for the organic fraction of municipal solid waste by De la Rubia et al. (2018a) under mesophilic conditions. At day 26, SCOD declined to 81% and 78% for PW200 and PW230, respectively (calculated referring to the initial SCOD at day 0). The non-biodegradable SCOD fraction could be attributed to refractory compounds (difficult to degrade) generated during food waste carbonization. Indeed, long-chain hydrocarbons and oxygen- and nitrogen-bearing aromatic compounds were detected in both process waters (Fig. 4).

The experimental cumulative methane yield was fitted with a first-order kinetic equation (Fig. 3), widely used to simulate methane production during AD (Marin-Batista et al., 2020b). Fitting was performed using Origin software (version 9.1). Considering the shape of the methane yield curve with no lag-phase, first-order kinetics were selected to simulate the CH<sub>4</sub> pattern during the AD test. The first-order kinetic equation (Eq. (8)) used to simulate CH<sub>4</sub> yield was:

$$G(t) = G_{max} \cdot [1 - \exp(-k \cdot t)] \quad (8)$$

where  $G_{max}$  (mL CH<sub>4</sub> STP g<sup>-1</sup> COD<sub>added</sub>) is the ultimate methane yield and  $k$  (d<sup>-1</sup>) is the kinetic constant.

### Figure 3

High values of determination coefficient  $R^2$  (0.998 for PW200 and 0.999 for PW230 and food waste) were observed, indicating a good fit of the experimental data to the proposed model. The predicted final methane yields were also close to the experimental ones. Values of  $G_{\max}$  (reported as modelled values  $\pm$  standard error) were:  $135 \pm 2$  mL  $\text{CH}_4$  STP  $\text{g}^{-1}$   $\text{COD}_{\text{added}}$  for PW200,  $150 \pm 2$  mL  $\text{CH}_4$  STP  $\text{g}^{-1}$   $\text{COD}_{\text{added}}$  for PW230 and  $229 \pm 1$  mL  $\text{CH}_4$  STP  $\text{g}^{-1}$   $\text{COD}_{\text{added}}$  for food waste. The specific rate constants ( $k$ ) of process water were similar ( $0.105 \pm 0.011$  and  $0.106 \pm 0.008$   $\text{d}^{-1}$  for PW200 and PW230, respectively). These values of  $k$  were higher than the kinetic constants described for process water obtained by HTC of sewage sludge ( $0.031$ – $0.048$   $\text{d}^{-1}$ ) (Villamil et al., 2018). For both process waters, all fitted parameters were comparable, sustaining the idea that there were no relevant differences between the two runs. For food waste, a comparable value of kinetic constant  $k$  ( $0.110 \pm 0.006$   $\text{d}^{-1}$ ) was obtained. Since no significant lag-phase was observed, it suggests that hydrolysis was not the limiting step in AD. The value of the first order constant was consistent with the range of  $k$  values ( $0.056$ – $0.364$   $\text{d}^{-1}$ ) reported elsewhere for AD of food waste using a different inoculum (Browne and Murphy, 2013). The raw food waste, PW200 and PW230 showed similar values of the kinetic constant, and both process waters resulted in a lower  $G_{\max}$  value than that estimated for food waste, which proved its higher biodegradability under anaerobic conditions compared to process waters. This may be due to recalcitrant compounds in HTC process water (Fig. 4), which could affect degradation.

Since carbonization reaction routes include hydrolysis, dehydration, decarboxylation, condensation, polymerization and aromatization, process water from HTC usually contains alkenes, phenolic and aromatic compounds (Danso-Boateng et al., 2015). A

semi-quantitative analysis of chemical compounds was therefore carried out on PW200 and PW230, before (day 0) and after AD (day 56). The species were assembled into chemical groups (i.e., long-chain hydrocarbons, pyrazine, pyridine, aromatic compounds including all aromatics not grouped in the above categories, and non-aromatic N-compounds). Their concentrations were expressed as chromatogram peak area (%). Fig. 4 shows the chemical species detected by GC/MS in the two process waters. In particular, PW200 showed a significantly higher percentage of long-chain hydrocarbons than PW230 at day 0. At the beginning of AD, PW200 was found to contain long-chain fatty acids with a methyl ester group (e.g., methyl ester hexadecanoic acid), whereas only 2-hexene was observed in PW230. This suggests that the lower temperature 200°C promotes long-chain hydrocarbons, which formed other compounds at 230°C. Ring-type structures with one or two N heteroatoms were found in both at the beginning of AD. Aromatics (e.g., 1,4-benzenediamine), pyrazines (e.g., 2-ethyl-3-methylpyrazine) and pyridines (e.g., 2-methylpyridine) were observed in both process water samples. These compounds are generally formed during HTC by hydrolysis of proteins and carbohydrates (Marin-Batista et al., 2020a). In addition, PW200 showed a lower percentage of aromatics than PW230 at day 0, suggesting that the higher temperature may promote aromaticity. After AD, both process waters showed a heterogeneous composition of long-chain hydrocarbons, aromatics and N-structures. Interestingly, the removal of specific compounds was observed in both runs. As reported in Supplementary information (Table S2), up to 74% and 67% of 2-methylpyridine was removed by day 56 from PW200 and PW230, respectively. In addition, removal of 2-ethyl-3-methylpyrazine was up to 93% and 83% for PW200 and PW230, respectively, indicating that AD may remove these specific compounds.

Finally, 2-methylcyclopentanone was detected in both runs at the end of the AD experiments, suggesting that this compound may be formed during anaerobic digestion.

#### Figure 4

### 3.3. Energy and economic evaluation of the HTC-AD coupled process

In order to compare the performance of HTC of food waste coupled with AD of the resulting process water with the standalone AD configuration, an energy balance was performed for the different process conditions (Table 3). The balance was performed starting from 1 kg of food waste (dry basis) with a moisture content of ~ 93 wt.%, according to the experimental data. In addition, solid and liquid yields obtained experimentally for the different operating conditions were considered. The energy input ( $E_{input}$ ) for AD was ignored in all cases due to mesophilic conditions. The destination of the AD effluent will depend on its characteristics. Therefore, several options could be considered, such as direct discharge into a waterbody or into an urban sewerage system to complete water treatment. On the contrary, the energy input for HTC of food waste required initial heating of the HTC reactor (1.5 m<sup>3</sup>) for 1 h to the selected HTC temperature, after loading the wet food waste at room temperature (25°C): about 24 MJ kg<sup>-1</sup><sub>dry feedstock</sub> in both cases. However, as this process is designed to work continuously, we integrated the energy of the streams for heat recovery. We assumed that the hot outlet stream from the HTC reactor could be used to preheat the inlet to 100°C, so the only energy input required was that needed to heat the feedstock. This reduced the energy requirements to maintain the process by more than 70% for both HTC temperatures. Energy inputs were calculated using Eq. (9) and (10):

$$E_{HTC,in} = [(m_L \cdot C_L + m_s \cdot C_{FW} + C_R + h_R \cdot A \cdot \tau) \cdot (T_{HTC} - T_{298K})] \quad (9)$$

$$E_{preheat-HTC,in} = [m_L \cdot C_L + m_s \cdot C_{FW}] \cdot (T_{HTC} - T_{373K}) \quad (10)$$

where  $m_L$  is the liquid content of the food waste;  $C_L$  the specific heat of the liquid fraction of food waste, assumed equal to water ( $4.18 \text{ kJ kg}^{-1} \text{ K}^{-1}$ );  $m_s$  the dry solid content of food waste;  $C_{FW}$  the specific heat of food waste ( $2.8 \text{ kJ kg}^{-1} \text{ K}^{-1}$ ), calculated with the Aspen Plus simulator using its experimental characteristics;  $C_R$  the heat capacity of the reactor ( $1550 \text{ kJ K}^{-1}$ );  $h_R$  the convective heat transfer coefficient;  $A$  the surface area of the HTC reactor ( $h_R \cdot A = 0.032 \text{ kW K}^{-1}$ ) (Namioka et al., 2008); and  $\tau$  the reaction time (1 h).

After carbonization of food waste, the hydrochar was assumed to be dewatered to a wet solid with a moisture content of 40 wt.% using a filter-press, and then thermally dried to reach a moisture content of around 8 wt.%. (Lucian et al., 2020; Yoshikawa and Prawisudha, 2014). Energy consumption for hydrochar dewatering was  $0.2 \text{ MJ kg}^{-1}$  of dry food waste in all cases, using  $162 \text{ kJ kg}^{-1}$  of the resulting solid as reference value (Lucian et al., 2020). The energy input for thermal drying was calculated on the basis of the steam required to evaporate the water ( $1.2 \text{ kg steam}$  (with an enthalpy of  $2631 \text{ kJ kg}^{-1}$  at 4 bar) per kg of water) from the wet hydrochar (Werther, 2009). It turned out to be 10% higher at  $200^\circ\text{C}$  than at  $230^\circ\text{C}$  due to the greater amount of solid generated. Finally,  $0.1 \text{ MJ kg}^{-1}$  of dry feedstock was allowed for hydrochar pelletization in both cases in order to facilitate its transport and use in heating systems;  $0.18 \text{ MJ kg}^{-1}$  was the reference value used (Lucian and Fiori, 2017). This means that the main energy requirement for the HTC system in preheating configuration was that of the HTC reaction (77% and 83% at  $200^\circ\text{C}$  and  $230^\circ\text{C}$ , respectively).



A value of  $18.9 \text{ MJ kg}^{-1}$  of dried food waste was taken as reference for the maximum heating value that this feedstock could provide by combustion. However, direct use of food waste as solid fuel is not recommended due to the high energy requirements for drying ( $2.5\text{--}2.7 \text{ MJ kg}^{-1}$  of evaporated water) (Fluck and Baird, 1980), in addition to the high N and S content compared to woody biomass, and the lower HHV (Kratzeisen et al., 2010). Furthermore, the use of raw food waste as a fuel is problematic because of its heterogeneity, low mass and low energy density (Pradhan et al., 2018).

The energy output ( $E_{\text{output}}$ ) of conventional AD depends on the amount of methane produced per kg of food waste. Therefore, since the potential energy output of AD is the entire net energy ( $E_{\text{output}} - E_{\text{input}}$ ), the energy recovery yield can be up to 67% of the feedstock energy content. This was mainly due to the high methane production of this substrate ( $228 \text{ mL STP CH}_4 \text{ g}^{-1} \text{ COD}_{\text{added}}$  or  $301 \text{ mL STP CH}_4 \text{ g}^{-1} \text{ VS}_{\text{added}}$ ). These values are comparable with those reported in the literature, the range of which is wide, depending on substrate characteristics ( $158\text{--}529 \text{ mL CH}_4 \text{ g}^{-1} \text{ VS}_{\text{added}}$ ) (Browne and Murphy, 2013). On the other hand, the total energy output of the combined HTC-AD process includes combustion of the hydrochar and the methane from AD of process water, which were at least 35% higher than the energy produced by AD alone for the two HTC temperatures. The energy output of HTC at  $230^\circ\text{C}$  was  $\sim 95\%$  of the energy available in the feedstock, which was around 5% higher than that obtained for HTC at  $200^\circ\text{C}$ . This is mainly due to the higher HHV of HC230, the greater amount of process water and the higher methane yield at this temperature. However, the net energy of HTC-AD depends on the energy inputs, and although the results remained positive, it is an energetically less favorable treatment (52% and 49% energy recovery at  $200^\circ\text{C}$  and  $230^\circ\text{C}$ , respectively) than AD of the feedstock. Nevertheless, HTC could play a key role

in food waste management. Indeed, despite the energy requirements of HTC-AD, this treatment can avoid generation of a large amount of unstable digestate by AD ( $\sim 0.5 \text{ ton ton}^{-1}_{\text{wet waste}}$  (Møller et al., 2009)). In addition, the energy requirements of HTC-AD can be covered by combustion of the methane and part of the hydrochar produced, while the excess can be marketed.

Although this study was mainly focused on energy recovery without going into economic aspects, product prices were taken into account. Thus, we assumed a natural gas selling price of  $2.01 \text{ € GJ}^{-1}$  (the average price in 2020 according to the U.S. Energy Information Administration), while the price of hydrochar was based on the market price established by Ingelia S.L. ( $9 \text{ € GJ}^{-1}$ ), which is also comparable to the price range of wood pellets ( $10\text{--}12 \text{ € GJ}^{-1}$ ) (De Mena Pardo et al., 2016). Assuming these market prices, it was possible to calculate an economic value for each process. As shown in Table 3, the treatment providing the highest economic value was HTC from food waste at  $200^\circ\text{C}$  coupled with AD of process water. In this case, the economic value proved to be three times that obtained with standalone AD.

### **Table 3**

## **4. Conclusions**

Hydrothermal carbonization emerges as alternative for valorizing food waste. Temperatures above  $200^\circ\text{C}$  were suitable for improving the energetic properties of hydrochar, which has attractive characteristics (HHV and combustion properties) as a biofuel for industry. Process water is valorized by anaerobic digestion, achieving promising methane production. Although the energy assessment is strongly influenced by the energy requirements for carbonization, HTC could offer real benefits in terms of

resources, particularly with regard to economic aspects. Considering the net energy and the subsequent economic value of both processes, AD coupled with HTC at 200°C seems to be optimal for food waste valorization.

## **Supplementary information**

Supplementary data of this article can be found in the online version.

## **Acknowledgments**

The authors acknowledge funding from the Spanish MICINN (Project PID2019-108445RB-I00) and Madrid Regional Government (Project S2018/EMT-4344). A. Sarrión thanks the Spanish MICINN and the ESF for a research grant (BES-2017-081515). G. Mannarino thanks the Tuscany Region for “Pegaso” fellowship.

## **References**

- Akarsu, K., Duman, G., Yilmazer, A., Keskin, T., Azbar, N., Yanik, J., 2019. Sustainable valorization of food wastes into solid fuel by hydrothermal carbonization. *Bioresour. Technol.* 292, 121959. <https://doi.org/10.1016/j.biortech.2019.121959>
- APHA, 2005. Standard methods for examination of water and wastewater, 21st ed. American Public Health Association/American Water Works Association/Water Environment Federation, Washington DC.
- Aragón-Briceño, C., Ross, A.B., Camargo-Valero, M.A., 2017. Evaluation and comparison of product yields and bio-methane potential in sewage digestate following hydrothermal treatment. *Appl. Energy* 208, 1357–1369. <https://doi.org/10.1016/j.apenergy.2017.09.019>

590 Browne, J.D., Murphy, J.D., 2013. Assessment of the resource associated with  
 591 biomethane from food waste. *Appl. Energy* 104, 170–177.  
 592 <https://doi.org/10.1016/j.apenergy.2012.11.017>

593 Channiwala, S.A., Parikh, P.P., 2002. A unified correlation for estimating HHV of  
 594 solid, liquid and gaseous fuels. *Fuel* 81, 1051–1063.  
 595 [https://doi.org/10.1016/S0016-2361\(01\)00131-4](https://doi.org/10.1016/S0016-2361(01)00131-4)

596 Dai, L., Yang, B., Li, H., Tan, F., Zhu, N., Zhu, Q., He, M., Ran, Y., Hu, G., 2017. A  
 597 synergistic combination of nutrient reclamation from manure and resultant  
 598 hydrochar upgradation by acid-supported hydrothermal carbonization.  
 599 *Bioresour. Technol.* 243, 860–866.  
 600 <https://doi.org/10.1016/j.biortech.2017.07.016>

601 Danso-Boateng, E., Shama, G., Wheatley, A.D., Martin, S.J., Holdich, R.G., 2015.  
 602 Hydrothermal carbonization of sewage sludge: Effect of process conditions on  
 603 product characteristics and methane production. *Bioresour. Technol.* 177, 318–  
 604 327. <https://doi.org/10.1016/j.biortech.2014.11.096>

605 De la Rubia, M.A., Villamil, J.A., Rodriguez, J.J., Borja, R., Mohedano, A.F., 2018a.  
 606 Mesophilic anaerobic co-digestion of the organic fraction of municipal solid  
 607 waste with the liquid fraction from hydrothermal carbonization of sewage  
 608 sludge. *Waste Manag.* 76, 315–322.  
 609 <https://doi.org/10.1016/j.wasman.2018.02.046>

610 De la Rubia, M.A., Villamil, J.A., Rodriguez, J.J., Mohedano, A.F., 2018b. Effect of  
 611 inoculum source and initial concentration on the anaerobic digestion of the  
 612 liquid fraction from hydrothermal carbonisation of sewage sludge. *Renew.*

Energy 127, 697–704. <https://doi.org/10.1016/j.renene.2018.05.002>

De Mena Pardo, B., Doyle, L., Renz, M., Salimbeni, A., 2016. Industrial scale hydrothermal carbonization: new applications for wet biomass waste. Ttz Bremerhaven: Bremerhaven, Germany.

European Commission, 2020. A new circular economy action plan for a cleaner and more competitive Europe. Brussels. <https://www.un.org/sustainabledevelopment/sustainable-consumption-production/> (accessed on 16 April 2021)

Fluck, R.C., Baird, C.D., 1980. Energy requirements for agricultural inputs in agricultural energetics, First. ed. AVI Publishing Company, Westport, Conn.

Funke, A., Ziegler, F., 2010. Hydrothermal carbonization of biomass: A summary and discussion of chemical mechanisms for process engineering. Biofuels, Bioprod. Biorefining 6, 246–256. <https://doi.org/10.1002/bbb>

Gupta, D., Mahajani, S.M., Garg, A., 2020. Investigation on hydrochar and macromolecules recovery opportunities from food waste after hydrothermal carbonization. Sci. Total Environ. 749, 142294. <https://doi.org/10.1016/j.scitotenv.2020.142294>

He, C., Giannis, A., Wang, J., 2013. Conversion of sewage sludge to clean solid fuel using hydrothermal carbonization: hydrochar fuel characteristics and combustion behaviour. Appl. Energy 111, 257–266. <https://doi.org/10.1016/j.apenergy.2013.04.084>

He, C., Zhang, Z., Ge, C., Liu, W., Tang, Y., Zhuang, X., Qiu, R., 2019. Synergistic effect of hydrothermal co-carbonization of sewage sludge with fruit and agricultural wastes on hydrochar fuel quality and combustion behavior. Waste

Manag. 100, 171–181. <https://doi.org/10.1016/J.WASMAN.2019.09.018>

Idowu, I., Li, L., Flora, J.R.V., Pellechia, P.J., Darko, S.A., Ro, K.S., Berge, N.D.,  
2017. Hydrothermal carbonization of food waste for nutrient recovery and reuse.  
Waste Manag. 105, 566–574. <https://doi.org/10.1016/j.wasman.2017.08.051>

Jenkins, S.R., Morgan, J.M., Sawyer, C.L., 1983. Measuring anaerobic sludge  
digestion and growth by a simple alkalimetric titration 55, 448–453

Kratzeisen, M., Starcevic, N., Martinov, M., Maurer, C., Müller, J., 2010.  
Applicability of biogas digestate as solid fuel. Fuel 89, 2544–2548.  
<https://doi.org/10.1016/j.fuel.2010.02.008>

Lang, Q., Zhang, B., Liu, Z., Chen, Z., Xia, Y., Li, D., Ma, J., Gai, C., 2019. Co-  
hydrothermal carbonization of corn stalk and swine manure: Combustion  
behavior of hydrochar by thermogravimetric analysis. Bioresour. Technol. 271,  
75–83. <https://doi.org/10.1016/j.biortech.2018.09.100>

Li, L., Flora, J.R.V., Berge, N.D., 2020. Predictions of energy recovery from  
hydrochar generated from the hydrothermal carbonization of organic wastes.  
Renew. Energy 145, 1883–1889. <https://doi.org/10.1016/j.renene.2019.07.103>

Liu, S., Wang, Y., Guo, J., Wang, W., Dong, R., 2021. Start-up and performance  
evaluation of upflow anaerobic sludge blanket reactor treating supernatant of  
hydrothermally treated municipal sludge: Effect of initial organic loading rate.  
Biochem. Eng. J. 166, 107843. <https://doi.org/10.1016/j.bej.2020.107843>

Lu, X., Jordan, B., Berge, N.D., 2012. Thermal conversion of municipal solid waste  
via hydrothermal carbonization: Comparison of carbonization products to  
products from current waste management techniques. Waste Manag. 32, 1353–  
1365. <https://doi.org/10.1016/j.wasman.2012.02.012>

Lucian, M., Volpe, M., Merzari, F., Wüst, D., Kruse, A., Andreottola, G., Fiori, L.,  
 2020. Hydrothermal carbonization coupled with anaerobic digestion for the  
 valorization of the organic fraction of municipal solid waste. *Bioresour.*  
*Technol.* 314, 123734. <https://doi.org/10.1016/j.biortech.2020.123734>

Lucian, M., Fiori, L., 2017. Hydrothermal carbonization of waste biomass: Process  
 design, modeling, energy efficiency and cost analysis. *Energies* 10.  
<https://doi.org/10.3390/en10020211>

Marin-Batista, J.D., Mohedano, A.F., Rodríguez, J.J., De la Rubia, M.A., 2020a.  
 Energy and phosphorous recovery through hydrothermal carbonization of  
 digested sewage sludge. *Waste Manag.* 105, 566–574.  
<https://doi.org/10.1016/j.wasman.2020.03.004>

Marin-Batista, J.D., Villamil, J.A., Qaramaleki, S. V., Coronella, C.J., De la Rubia,  
 M.A., 2020b. Energy valorization of cow manure by hydrothermal carbonization  
 and anaerobic digestion. *Renew. Energy* 160, 623–632.  
<https://doi.org/10.1016/j.renene.2020.07.003>

Møller, J., Boldrin, A., Christensen, T.H., 2009. Anaerobic digestion and digestate  
 use: Accounting of greenhouse gases and global warming contribution. *Waste*  
*Manag. Res.* 27, 813–824. <https://doi.org/10.1177/0734242X09344876>

Mureddu, M., Dessi, F., Orsini, A., Ferrara, F., Pettinau, A., 2018. Air- and oxygen-  
 blown characterization of the coal and biomass by thermogravimetric analysis.  
*Fuel* 212, 626–637. <https://doi.org/10.1016/j.fuel.2017.10.005>

Namioka, T., Miyazaki, M., Morohashi, Y., Umeki, K., Yoshikawa, K., 2008.  
 Modeling and analysis of batch-type thermal sludge pretreatment for optimal  
 design. *J. Environ. Eng.* 3, 170–181. <https://doi.org/10.1299/jee.3.170>

- Niu, S., Chen, M., Li, Y., Xue, F., 2016. Evaluation on the oxy-fuel combustion behavior of dried sewage sludge. *Fuel* 178, 129–138.  
<https://doi.org/10.1016/j.fuel.2016.03.053>
- Pham, T.P.T., Kaushik, R., Parshetti, G.K., Mahmood, R., Balasubramanian, R., 2015. Food waste-to-energy conversion technologies: Current status and future directions. *Waste Manag.* 38, 399–408.  
<https://doi.org/10.1016/j.wasman.2014.12.004>
- Pradhan, P., Mahajani, S.M., Arora, A., 2018. Production and utilization of fuel pellets from biomass: A review. *Fuel Process. Technol.* 181, 215–232.  
<https://doi.org/10.1016/j.fuproc.2018.09.021>
- Raposo, F., de la Rubia, M.A., Borja, R., Alaiz, M., 2008. Assessment of a modified and optimised method for determining chemical oxygen demand of solid substrates and solutions with high suspended solid content. *Talanta* 76, 448–453.  
<https://doi.org/10.1016/j.talanta.2008.03.030>
- Reza, M.T., Lynam, J.G., Uddin, M.H., Coronella, C.J., 2013. Hydrothermal carbonization: Fate of inorganics. *Biomass Bioenerg* 49, 86–94.  
<https://doi.org/https://doi.org/10.1016/j.biombioe.2012.12.004>
- Ro, K.S., Libra, J.A., Bae, S., Berge, N.D., Flora, J.R.V., Pecenka, R.: Combustion Behavior of Animal-Manure-Based Hydrochar and Pyrochar. *ACS Sustain. Chem. Eng.* 7, 470–478 (2019). <https://doi.org/10.1021/acssuschemeng.8b03926>
- Sahu, S.G., Sarkar, P., Chakraborty, N., Adak, A.K., 2010. Thermogravimetric assessment of combustion characteristics of blends of a coal with different biomass chars. *Fuel Process. Technol.* 91, 369–378.  
<https://doi.org/10.1016/j.fuproc.2009.12.001>



- Saqib, N.U., Sharma, H.B., Baroutian, S., Dubey, B., Sarmah, A.K., 2019. Valorisation of food waste via hydrothermal carbonisation and techno-economic feasibility assessment. *Sci. Total Environ.* 690, 261–276. <https://doi.org/10.1016/j.scitotenv.2019.06.484>
- Sarrion, A., Diaz, E., de la Rubia, M.A., Mohedano, A.F., 2021. Fate of nutrients during hydrothermal treatment of food waste. *Bioresour. Technol.* 342, 125954. <https://doi.org/10.1016/J.BIORTECH.2021.125954>
- Smith, A.M., Ross, A.B., 2016. Production of bio-coal, bio-methane and fertilizer from seaweed via hydrothermal carbonisation. *Algal Res.* 16, 1–11. <https://doi.org/10.1016/j.algal.2016.02.026>
- U.S. Energy information administration, 2020. Henry Hub Natural Gas Spot Price. <https://www.eia.gov/dnav/ng/hist/rngwhhdA.htm> (accessed on 16 April 2021)
- Villamil, J.A., Mohedano, A.F., Rodriguez, J.J., de la Rubia, M.A., 2018. Valorisation of the liquid fraction from hydrothermal carbonisation of sewage sludge by anaerobic digestion. *J. Chem. Technol. Biotechnol.* 93, 450–456. <https://doi.org/10.1002/jctb.5375>
- Wang, L., Chang, Y., Liu, Q., 2019. Fate and distribution of nutrients and heavy metals during hydrothermal carbonization of sewage sludge with implication to land application. *J. Clean. Prod.* 225, 972–983. <https://doi.org/10.1016/j.jclepro.2019.03.347>
- Wang, T., Zhai, Y., Zhu, Y., Gan, X., Zheng, L., Peng, C., Wang, B., Li, C., Zeng, G., 2018. Evaluation of the clean characteristics and combustion behavior of hydrochar derived from food waste towards solid biofuel production. *Bioresour. Technol.* 266, 275–283. <https://doi.org/10.1016/j.biortech.2018.06.093>

- Weide, T., Brüggling, E., Wetter, C., 2019. Anaerobic and aerobic degradation of wastewater from hydrothermal carbonization (HTC) in a continuous, three-stage and semi-industrial system. *J. Environ. Chem. Eng.* 7. <https://doi.org/10.1016/j.jece.2019.102912>
- Werther, J., 2009. Potentials of biomass co-combustion in coal-fired boilers, in: *Proceedings of the 20th International Conference on Fluidized Bed Combustion*. SpringerOpen, pp. 27–42. [https://doi.org/10.1007/978-3-642-02682-9\\_3](https://doi.org/10.1007/978-3-642-02682-9_3)
- Wirth, B., Reza, T., Mumme, J., 2015. Influence of digestion temperature and organic loading rate on the continuous anaerobic treatment of process liquor from hydrothermal carbonization of sewage sludge. *Bioresour. Technol.* 198, 215–222. <https://doi.org/10.1016/j.biortech.2015.09.022>
- Yoshikawa, K., Prawisudha, P., 2014. *Hydrothermal Treatment of Municipal Solid Waste for Producing Solid Fuel*. Springer, Berlin, Heidelberg, pp. 355–383. [https://doi.org/10.1007/978-3-642-54458-3\\_14](https://doi.org/10.1007/978-3-642-54458-3_14)
- Zheng, C., Ma, X., Yao, Z., Chen, X., 2019. The properties and combustion behaviors of hydrochars derived from co-hydrothermal carbonization of sewage sludge and food waste. *Bioresour. Technol.* 285, 121347. <https://doi.org/10.1016/j.biortech.2019.121347>

752  
753

**Table 1.** Representative analysis of food waste and hydrochar (dry basis).

Sample	Proximate analysis (wt.%)				Ultimate analysis (wt.%)					HHV (MJ kg <sup>-1</sup> )	Mineral elements (wt.%)						
	Yield	FC	VM	Ash	C	N	S	H	O <sup>a</sup>		Na	K	Ca	Mg	Fe	Al	P
Food waste	-	11.0	77.2	11.8	44.5	3.1	0.2	6.1	34.3	18.9	0.14	3.30	1.17	0.23	0.11	0.10	0.47
		(0.2)	(0.1)	(0.1)	(0.3)	(0.2)	(0.0)	(0.8)	(0.2)	(0.1)	(0.01)	(0.03)	(0.02)	(0.01)	(0.02)	(0.04)	(0.03)
HC200	64.5	28.6	57.8	13.6	48.6	2.0	0.2	5.7	29.9	20.3	0.23	3.67	1.57	0.31	0.29	0.25	0.57
		(0.2)	(0.4)	(1.6)	(0.2)	(0.3)	(0.2)	(0.0)	(0.2)	(0.2)	(0.02)	(0.03)	(0.06)	(0.02)	(0.01)	(0.04)	(0.02)
HC230	58.3	29.5	56.2	14.3	54.8	2.3	0.2	6.1	22.3	23.7	0.10	1.61	1.88	0.29	0.33	0.40	0.83
		(1.6)	(0.9)	(0.2)	(0.2)	(0.9)	(0.3)	(0.0)	(0.1)	(0.1)	(0.01)	(0.02)	(0.03)	(0.01)	(0.01)	(0.03)	(0.04)

754

<sup>a</sup> Calculated by difference O = 100 - (C+H+N+S+Ash). Standard deviation is reported in brackets.

755

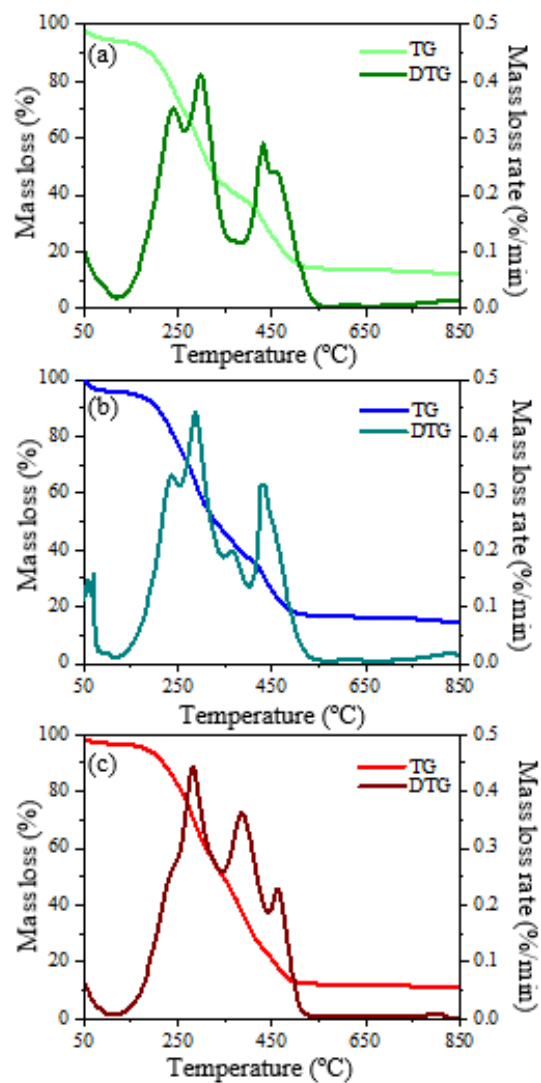


**Fig. 1.** TG and DTG curves of raw food waste (a), HC200 (b) and HC230 (c).

**Table 2.** Characterization of PW from HTC on food waste at 200 and 230 °C.

	<b>PW200</b>	<b>PW 230</b>
<b>TS (g L<sup>-1</sup>)</b>	38.8 (0.8)	35.9 (0.3)
<b>VS (g L<sup>-1</sup>)</b>	30.4 (0.9)	28.0 (0.4)
<b>SCOD (g O<sub>2</sub> L<sup>-1</sup>)</b>	68.2 (1.5)	62.4 (1.5)
<b>TOC (g L<sup>-1</sup>)</b>	24.3 (0.5)	23.6 (0.5)
<b>TN (g L<sup>-1</sup>)</b>	1.8 (0.1)	1.8 (0.1)
<b>TP (mg L<sup>-1</sup>)</b>	40.7 (0.1)	12.6 (0.1)
<b>pH</b>	3.9 (0.1)	3.8 (0.1)

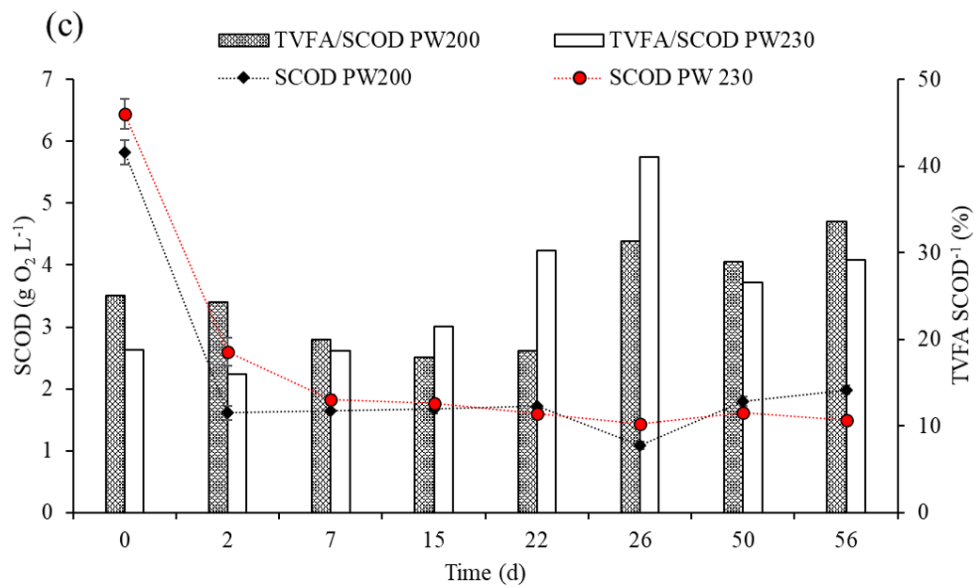
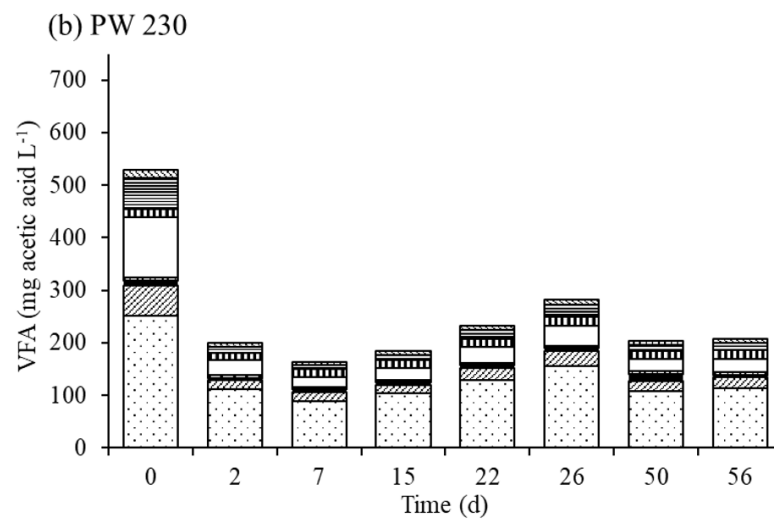
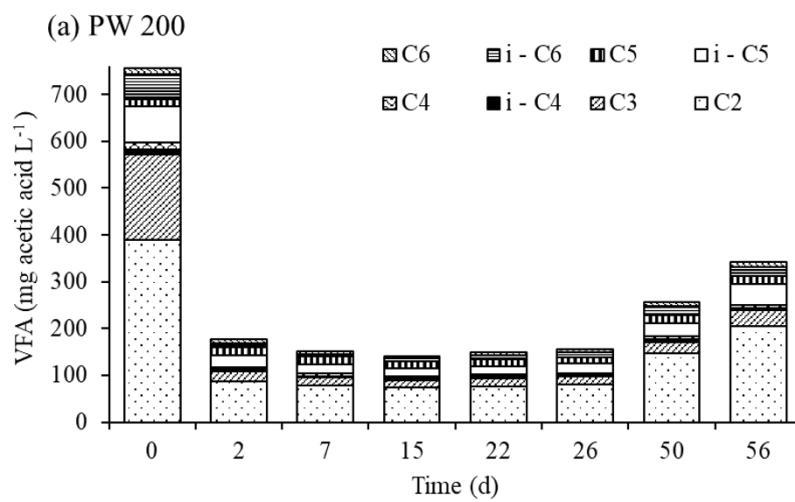


**Fig. 2.** Time-course of individual VFA concentrations (in mg acetic acid L<sup>-1</sup>) during anaerobic digestion for (a) PW200 and (b) PW230; (c) time-course of SCOD (in g O<sub>2</sub> L<sup>-1</sup>) and TVFA/SCOD ratio (%) (both parameters expressed as g O<sub>2</sub> L<sup>-1</sup>) during anaerobic digestion of process water from HTC of food waste.

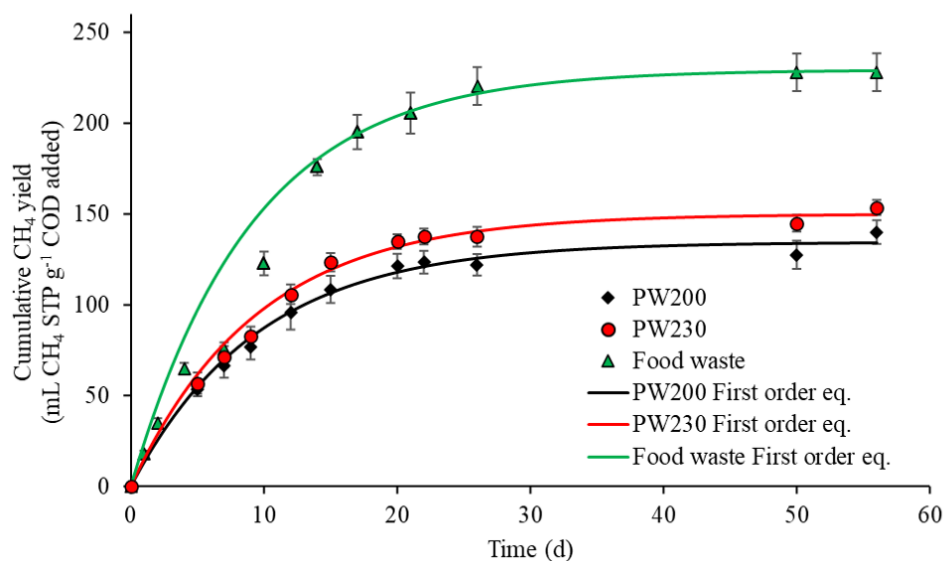


**Fig. 3.** Time-course of cumulative methane yield from food waste, PW200 and PW230 during anaerobic digestion (experimental data and first-order equation values).

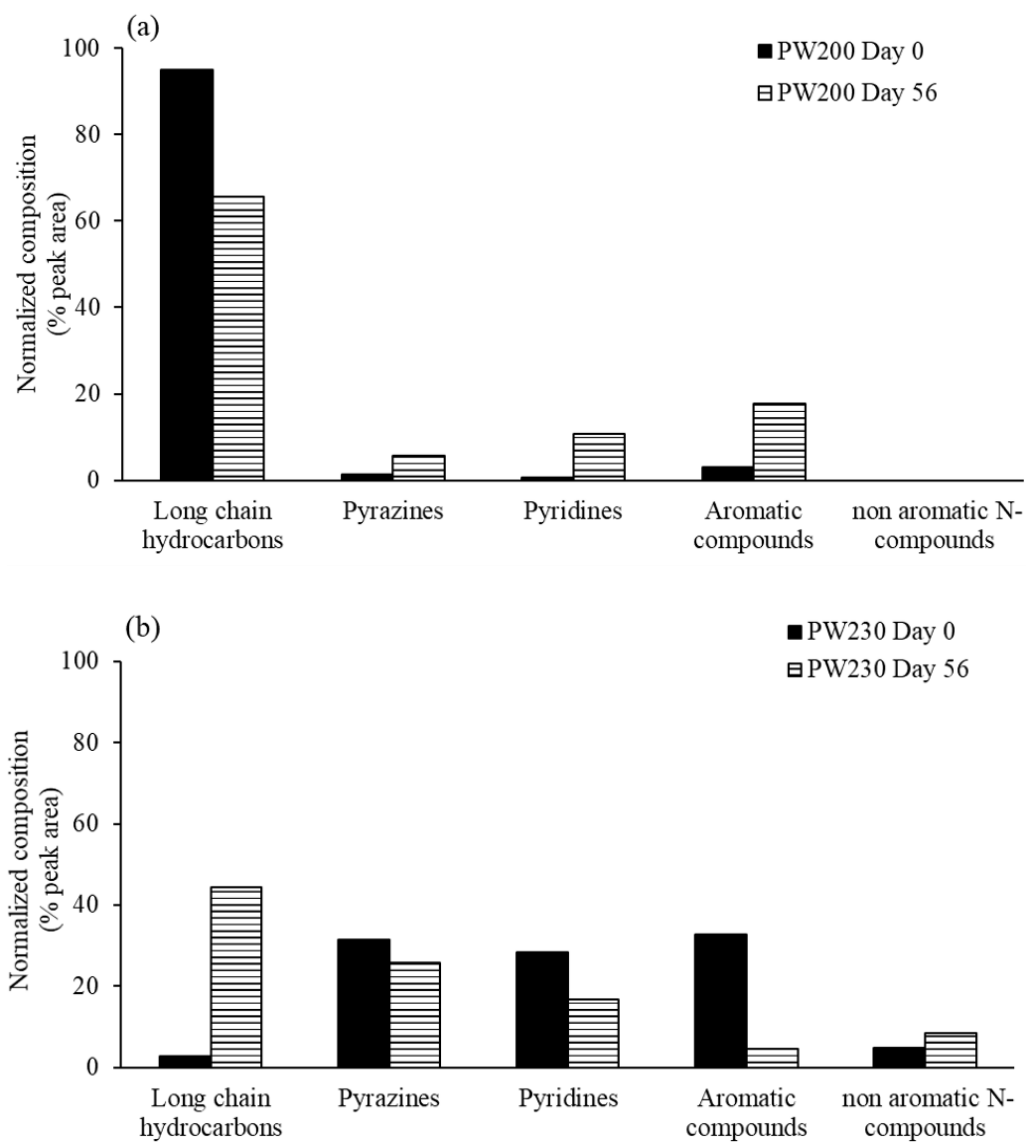


**Fig. 4.** Chemical species detected by GC/MS in (a) PW200 and (b) PW230 at Day 0 and Day 56 of anaerobic digestion.



865

**Table 3.** Energy and economic assessment of food waste valorization by AD and HTC-AD.

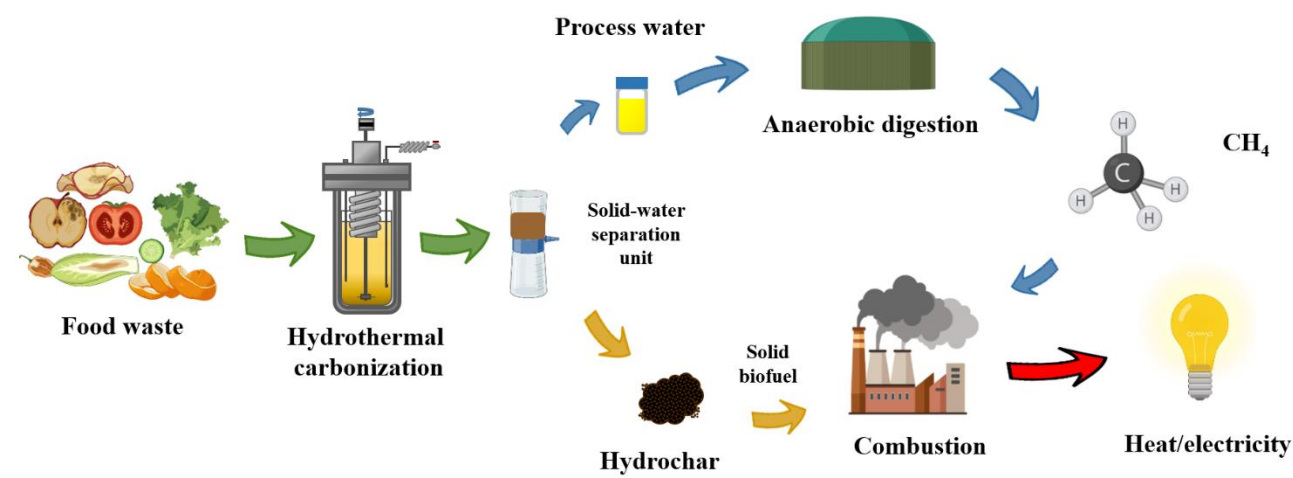
T (°C)		Energy Input (MJ kg <sup>-1</sup> dry feedstock)					Energy Output (MJ kg <sup>-1</sup> dry feedstock)			Economic value (€ kg <sup>-1</sup> dry feedstock) <sup>b</sup>
		HTC Reaction	Dewatering	Thermal drying	Pelletizer	Total input	Combustion		Total output	
Hydrochar	Methane									
HTC-	200	5.6	0.2	1.4	0.1	7.2	13.1	4.0	17.1	0.10
AD	230	7.3	0.2	1.2	0.1	8.8	13.8	4.2	18.0	0.08
AD	35	-	-	-	-	-	-	12.7	12.7	0.03

866

<sup>b</sup> from the sale of the excess product

867

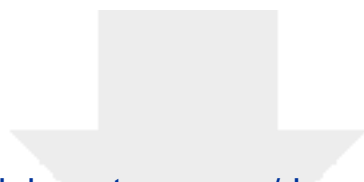
Graphical abstract



**Declaration of interests**

☒ The authors declare that they have no known competing financial interests or personal relationships that could have appeared to influence the work reported in this paper.

☐The authors declare the following financial interests/personal relationships which may be considered as potential competing interests:



[Click here to access/download](#)

**Supplementary Material**

Clean Supplementary Material\_02.docx

